Articles in PresS. J Neurophysiol (May 10, 2006). doi:10.1152/jn.00347.2006

JN-00347-2006

J. Neurophysiology (Innovative Methodology)
FINAL ACCEPTED VERSION

Title: # High-resolution multi-transistor array recording of electrical field potentials in cultured brain slices

Running title: Multi-transistor array recording in brain slices

Authors: M. Hutzler[1)]*, A. Lambacher[1)]*, B. Eversmann[2)], M. Jenkner[2)], R. Thewes[2)], and P. Fromherz[1)]

[1)] Max Planck Institute for Biochemistry, Department of Membrane and Neurophysics, Martinsried / Munich, and

[2)] Infineon Technologies, Corporate Research, Munich

*) *These authors contributed equally to the work.*

Correspondence: Peter Fromherz
Department of Membrane and Neurophysics
Max Planck Institute for Biochemistry
Martinsried / Munich, Germany 82152
Fone +49 89 8578 2820
Fax +49 89 8578 2822
fromherz@biochem.mpg.de

Abstract

We report on the recording of electrical activity in cultured hippocampal slices by a multi-transistor array (MTA) with 16384 elements. Time-resolved imaging is achieved with a resolution of 7.8 μm on an area of 1 mm^2 at 2 kHz. A read-out of fewer elements allows an enhanced time resolution. Individual transistor signals are caused by local evoked field potentials. They agree with micropipette measurements in amplitude and shape. The spatial continuity of the records provides time-resolved images of evoked field potentials and allows the detection of functional correlations over large distances. As examples, fast propagating waves of presynaptic action potentials are recorded as well as patterns of excitatory postsynaptic potentials across and along cornu ammonis.

Key words

multi-site recording, transistor recording, functional imaging, brain slice, rat hippocampus

Introduction

An understanding of brain tissue on the level of its neuronal networks requires stimulation and recording of electrical activity at a high spatiotemporal resolution over a large area of tissue. The ultimate aim is to elicit and detect the electrical excitation of every neuron in a functional area in order to observe correlations in space and time. Planar systems such as brain slices and retinae are particularly suitable for such an approach. There, metallic multi-electrode arrays (MEA) have been used to record extracellular field potentials (Jobling et al. 1981; Novak & Wheeler 1988; Meister et al. 1991; Stoppini et al. 1997; Egert et al. 1998; Duport et al. 1999; Jahnsen et al. 1999; Oka et al. 1999; Thiebaud et al. 1999; Gholmieh et al. 2001; Heuschkel et al. 2002; van Bergen et al. 2003; Segev et al. 2004). Their spatial resolution, however, is rather low or else restricted to a small area. Moreover, the records of extracellular potentials are distinctly smaller than measured with conventional micropipette electrodes. Another approach is optical recording with voltage-sensitive dyes in brain slices (Grinvald et al. 1982; Bonhoeffer et al. 1989; Nakagami et al. 1997; Matsukawa et al.; 2003; Grinvald & Hildesheim 2004; Mann et al. 2005). There, toxicity and unstable staining limit the duration of recording.

To overcome the problems, electrolyte-oxide-semiconductor (EOS) transistors have been introduced with cultured slices of rat hippocampus (Besl & Fromherz 2002; Hutzler & Fromherz 2004; Fromherz 2005). The EOS transistor signals matched micropipette recordings of field potentials. But a high resolution of 5 μm was achieved only in one dimension. Recently, high-density two-dimensional multi-transistor arrays (MTA) were implemented by an extended CMOS (complementary metal oxide

semiconductor) technology and tested with snail neurons (Eversmann et al. 2003; Lambacher et al. 2004).

In the present paper we demonstrate how MTA recording can be applied to cultured brain slices to yield time resolved images of electrical field potentials at a spatial resolution of 7.8 µm on an area of 1 mm^2. The total array is read out at a frequency of 2 kHz. Higher frequencies are attained by reading out part of the array. The principle of recording is illustrated in Figure 1. Brain tissue is in contact to an insulating and inert layer of TiO_2 that covers the silicon chip (Hutzler & Fromherz 2004; Wallrapp & Fromherz 2006). Integrated transistors are built in an electrolyte-oxide-metal-oxide-semiconductor (EOMOS) configuration: a local change of the electrical field potential is capacitively coupled through the insulating TiO_2 layer to the gate of a field-effect transistor. There it gives rise to a modulation of the source-drain current that is calibrated in terms of the field potential. The surface of a chip is shown in Figure 2: through the insulating TiO_2 we can see the 16384 contacts with a diameter of 4.5 µm and a pitch of 7.8 µm. Figure 3a shows that the MTA is able to cover a large part of a hippocampal slice where cornu ammonis and gyrus dentatus can be identified by comparison with the classical anatomical drawing in Figure 3b (Ramón y Cajal 1911).

Materials and Methods

Chips

The silicon chips have a size of 5.4 mm x 6.5 mm. Details of their design are described in previous publications (Eversmann et al. 2003; Lambacher et al. 2004). The

chips are wire bonded to standard ceramic packages. A chamber of perspex is attached to shield the bond contacts and to expose the transistor array to culture medium (Besl & Fromherz 2002; Lambacher et al. 2004). The chips are cleaned twice with detergent (BM flüssig, 104101; Biomed Labordiagnostik GmbH, Oberschleissheim, Germany), wiping them with cotton swabs, and rinsed with Milli-Q water. After drying and sterilization with UV light (30 min), we applied 400 µl of a solution of poly-L-lysine (P6516; Sigma, Deisenhofen, Germany) at 1 mg/ml in 0.13 M Tris/HCl buffer (pH 8.4) for 48 h, rinsed the chips with Milli-Q water and dried them. No change of chip quality was observed after five cleaning-culture-measurement cycles.

Hippocampal slice culture

Organotypic slices from rat hippocampus on silicon chips were prepared following established procedures (Gähwiler 1981; Debanne et al. 1999; Besl & Fromherz 2002). In short, the hippocampi of 5 to 7 day old Wistar rats were excised after decapitation and cut into 400 µm thick transverse slices using a McIlwain tissue chopper. They were transferred to 3 µl of chicken plasma (30-0390L, Cocalico Biologicals, Reamstown, USA) spread on the chip. The slice was gently placed onto the transistor array, using a pipette. Precise positioning was difficult due to capillar attraction of the plasma-immersed slice to the walls of the narrow chamber. Coagulation was started by adding 3 µl of thrombin solution (112374, Merck, 140 U/ml) that immobilized the slice on the chip. After 4 min, 1 ml of culture medium was added, consisting of 50% BME (21090-022, Invitrogen), 25% Hanks' balanced salt solution (24020-091, Invitrogen) and 25% horse serum (16050-122, Invitrogen) with 1 mM L-Glutamine (25030-032, Invitrogen) and 25 mM D-Glucose. The chamber was closed with the lid of a falcon dish (Falcon 3001; Becton Dickinson Labware Europe,

Le Pont De Claix, France) using seal and clip (Besl & Fromherz 2002), placed in an incubator (Incudrive-S; Schütt Labortechnik, Göttingen, Germany) at 34 °C and rotated at 10 rev/h. Three days after preparation, mitose inhibitors (uridine, U-3750, cytosine-β-D-arabino-furanoside, C-6645, 5-fluoro-2'-deoxyuridine, F-0503, Sigma) were added to a concentration of 10 μM. The culture medium was exchanged one day after the addition of the inhibitors and again one week later. The slices were cultured for 7-10 days.

A chip with slice was placed into the socket of the electronic set-up that was able to dissipate the heat created by the chip. The slice was perfused with recording medium at about 32°C with a rate of 1 ml/min. The recording medium (Debanne et al. 1999) contained (in mM) 149 Na^+, 149 Cl^-, 2.7 K^+, 2.8 Ca^{2+}, 2.0 Mg^{2+}, 11.6 HCO_3^-, 0.4 $H_2PO_4^-$ and 5.6 Glucose and was adjusted to pH 7.4 by titration with HCl. Excitatory synaptic transmission was blocked in some experiments by D-AP5 (D-(-)-2-Amino-5-phosphonopentanoic acid, 106-10, BioTrend GmbH, Köln, Germany) and DNQX (6,7-Dinitroquinoxaline-2,3-dione, D-0540, Sigma, from DMSO stock solution) both at a concentration of 50 μM (Davies & Watkins 1982; Honore et al. 1988).

Electrophysiology

For stimulation we used monopolar tungsten microelectrodes (AMS 5753, Science Products, Hofheim, Germany). A stimulus isolation unit (A360D, World Precision Instruments, Berlin, Germany) generated 200 μs negative current pulses of 50-70 μA. The bath electrolyte was held at a constant electrical potential with a Ag/AgCl pellet electrode (E-206, Science Products, Hofheim, Germany). Local electrical field potentials were measured with micropipette electrodes. The

micropipettes (tip diameter about 2 μm, resistance about 10 MΩ) were made from borosilicate glass (1403547, Hilgenberg, Germany), filled with 3M NaCl and contacted with a chlorinated silver wire. They were connected to an amplifier (BA-1S, NPI electronic, Tamm, Germany). The signals were bandpass filtered between 1 Hz and 1 kHz and sampled at 10 kHz. Tungsten electrode and micropipette were positioned with micromanipulators (Narishige, Tokyo, Japan).

MTA recording

Slices were stimulated with a tungsten microelectrode positioned in the pyramidal layer of the CA3 area. The electrical response was measured with 16384 sensor transistors. In some cases, we first performed an imaging experiment with standard recording medium, and subsequently with a medium containing the toxins DNQX (50 μM) and AP5 (50 μM) to block AMPA and NMDA channels and to observe presynaptic activity alone. Reversibility of toxin effects was confirmed by washout.

During a recording experiment, the columns of the transistor array were sequentially connected to 128 line amplifiers. After a settling time of 1.92 μs the output of these line amplifiers was multiplexed during another 1.92 μs into 16 output channels. The read-out time of the whole chip therefore was 492 μs. It could be shortened by restricting the read-out to a fraction of the array. The read-out scheme created a time gradient along the sensor area, as only 16 sensor transistors were read out at exactly the same time. We obtained isochronic images by interpolating the signals linearly between the two frames before and after the chosen time at each position.

The multiplexing scheme required a maximum on-chip bandwith of 32 MHz, far larger than allowed by the sampling theorem at the read-out frequency of

2 kHz. From the resulting aliasing together with the intrinsic noise of the sensor transistors (gate area 11 μm²) we expected a minimal noise around 50 μV rms. We observed a total noise of about 250 μV rms due to imperfections of chip design and set-up. In some experiments the signal-to-noise ratio was improved by spatial Gaussian filtering.

Due to the small size of the sensor transistors, there is a statistical variation of the threshold voltage with a standard deviation of 4.2 mV that is large compared to extracellular neuronal signals. A reset circuit is implemented on the chip that assigns individual bias voltages to the gates to maintain a common baseline (Eversmann et al. 2003; Lambacher et al. 2004). Reset cycles are applied until the start of a measurement. There is a minor drift of the working point within the duration of a measurement (590 ms). It is eliminated by fitting the transistor record before and after the interval of the evoked neuronal signals (about 40 ms) by a polynomial function that is subtracted from the complete record.

EOMOS transistors are calibrated by applying rectangular voltage pulses of 70 Hz and 5 mV peak to peak to the bath electrode. The calibration is performed for the same duration as the measurement to check for a drift of sensitivity. The voltage pulses give rise to a change of the electrical potential at the surface of the chip. The local change of electrical potential couples through the insulating electrolyte/chip interface to the top metal contact and to the gate of the transistor (Figure 1) and proportionally modulates the source-drain current.

In a measurement, the excited brain slice gives rise to a electrical field potential, i.e. to changes of the local extracellular voltage with respect to the bath electrode on

ground potential. The local field potential at the surface of the chip couples through the insulating electrolyte/chip interface to the gate and proportionally modulates the source-drain current as in the situation of calibration. Due to the design of the CMOS chip, there is no crosstalk of transistor signals on the chip. The response of a transistor is solely determined by the local field potential above the insulating TiO_2 averaged over the diameter of 4.5 μm of the top contact.

Results

Individual transistor signal

At first we consider a typical measurement by a single EOMOS transistor. Figure 4 shows a selected transistor record of an evoked field potential in stratum pyramidale in an area where the transistor records were almost invariant within a range of 20 μm. The slice is stimulated by a tungsten microelectrode in the pyramidal layer of CA3 with a negative current pulse of 55 μA and 200 μs in a region that was 1.2 mm apart from the site of recording along the arch of cornu ammonis. By reading out only part of the MTA, the transistor signals were recorded at an enhanced sampling rate of 8 kHz. In order to improve the signal-to-noise ratio, we applied a Bessel filtering between 1 Hz and 1 kHz and a twodimensional spatial Gaussian filtering with $\sigma = \sqrt{2}$ pixel (11 μm). Five milliseconds after the stimulation artifact, the transistor measured a positive voltage transient with an amplitude of 3 mV and a duration of about 20 ms.

Amplitude and shape of the signal are typical for a local electrical field potential in stratum pyramidale as measured by standard micropipette techniques (Johnston & Amaral 1998). It is caused by the activation of excitatory synapses (population

excitatory postsynaptic potential, pEPSP) in stratum radiatum. In all regions of stratum pyramidale and stratum radiatum that are probed by the MTA (see Figure 5), we find a similar shape and a similar amplitude of the EOMOS transistor signals and of common micropipette recordings in brain slices (Richardson et al. 1987, Duport et al. 1999). Thus the EOMOS transistors are able to record local field potentials.

For illustration, we impaled a micropipette into the cultured hippocampal slice and lowered its tip as closely as possible to the selected transistor without damaging chip and electrode. In the microscope, the lateral position of the tip could be identified up to about 20 μm. The micropipette signal that is simultaneously recorded with the EOMOS transistor signals is also plotted in Figure 4. It has a very similar shape with an amplitude of about 2 mV. The lower amplitude can be assigned to the different vertical position of the two probes: due to current flow from neuronal sources in the slice to the bath there is a drop of the field potential across the slice such that a micropipette records a lower signal than the transistor (Fromherz 2002).

Functional imaging

We consider one data set for time resolved imaging of electrical activity in a cultured hippocampal slice with the slice-chip system depicted in Figure 3a. We used all 16384 sensor transistors that were read out at 2 kHz. A movie of the complete measurement can be downloaded from the website of the journal. The results were reproducible for repeated stimulations of the same slice. Similar results of spatiotemporal dynamics were obtained in 12 further slice-chip systems with different positions of the cultured slice on the transistor array.

Presynaptic imaging. We consider first an imaging experiment in which toxins

block the synaptic transmission mediated by NMDA/AMPA type channels. Reversibility of the toxin effects was confirmed by washout. The left column of Figure 5 displays eight frames between 1 ms and 20 ms after stimulation with a tungsten microelectrode (negative current pulse of 70 μA and 200 μs) that was placed in the pyramidal layer of CA3 as shown in Figure 3a. In the frames recorded at 1, 1.5 and 2 ms after stimulation we observe distinct negative transients that propagated from the site of stimulation along cornu ammonis in two directions. At later phases (Figure 5, 5 ms), no field potentials are detected. So we exclude a significant contribution of postsynaptic signals due to GABA type channels that were not blocked.

We replotted a blow-up of a selected MTA record at 1.5 ms after stimulation in Figure 6a. A grey line marks the border between stratum pyramidale and stratum radiatum as it is derived from the functional image of postsynaptic activity without toxins in Figure 6b (see below). The picture shows that the fast wave of presynaptic activity is localized near stratum pyramidale. That localization indicates that the wave reflects action potentials that propagate along the mossy fibers that were stimulated by the tungsten microelectrode en passant (Andersen et al. 1971; Amaral & Witter 1989; Ishizuka et al. 1990). Accordingly, the orthodrome propagation terminates in a region of cornu ammonis where the border of CA3 and CA1 is located, and the antidrome propagation terminates near gyrus dentatus (Figure 5, left). From the frames at 1, 1.5 and 2 ms we evaluate a velocity of about 0.25 m/s, a typical value for the unmyelinated mossy fibers (Andersen et al. 1971).

In the last phase of the signal (frame 3 ms in Figure 5, left), we see a wave spreading into stratum radiatum. Considering the relation in space and time of that

signal with the precedent signal along stratum pyramidale, that wave indicates how mossy fibers invade the dendritic region of CA3.

With applied toxins, we were not able to see presynaptic activity that propagated from CA3 to CA1 along stratum radiatum where the Schaffer collaterals are localized in acute and cultured slices (Andersen et al. 1971; Amaral & Witter 1989; Ishizuka et al. 1990; Caesar & Aertsen 1991). The number of stimulated collaterals may have been too low in our experiment to give rise to a fiber volley with sufficiently high amplitude to be recorded by the MTA.

Postsynaptic imaging. Eight time frames of an MTA record without toxins are depicted in the right column of Figure 5. In the frames at 1 and 1.5 ms after stimulation, we see again negative transients that spread in two directions as in the experiment with toxins. But now, 2 ms after stimulation, additional negative and positive signals arise along cornu ammonis. The spread of the negative and positive wing is not perfectly synchronous. The signals fade away beyond 20 ms after stimulation. We assign these evoked field potentials to excitatory synaptic inwards currents in stratum radiatum and compensating outwards currents in stratum pyramidale (Johnston & Amaral 1998).

We replotted a blow-up of a selected MTA record at 5 ms after stimulation without toxin in Figure 6b. Due to their long duration, the postsynaptic signals are still visible near the stimulation site when their front reaches the boundaries of CA3. We marked the border between the positive and negative wing of the signals with a grey curve. For orientation, that line is also drawn in the micrograph of Figure 3a. It follows the structure of cornu ammonis. The MTA record at 5 ms after stimulation provides a perfect functional image of the hippocampal slice in terms of its postsynaptic activity.

We observed weak postsynapic signals downwards along cornu ammonis in the CA1 region with a negative amplitude in stratum radiatum and positive amplitude in stratum pyramidale (frames 5 ms and 10 ms, Figure 5, right). These signals may arise from an activation of CA3-CA1 synapses by Schaffer collaterals with an excitation that was too low to be recorded by the MTA.

Selected MTA recordings

Field potential across the layers. From the full set of data in Figure 5, we evaluated a linear profile of the field potential without toxins across the strata of CA3 as marked in Figure 6b at 5 ms after stimulation. The result is plotted in Figure 7. There is a wide trough in stratum radiatum and a narrower ridge in stratum pyramidale. For comparison, the profile with toxins 2.5 ms after stimulation at the same position is also shown in Figure 7. Only a shallow trough is observed in stratum pyramidale. Qualitatively, the profile without toxin reflects the inward current through glutamate receptors in the dendrites and compensating outward currents in the somata (Richardson et al. 1987; Johnston & Amaral 1998).

Field potential along the layers. Commonly, the functional features of the hippocampus are assumed to change little in transverse direction along the strata of CA3 or CA1 (Johnston & Amaral 1998). The twodimensional representation of the field potential in Figure 5 (right, 5 ms) indicates, however, that the postsynaptic signal is not homogeneous along stratum pyramidale of CA3, but that there is a distinct positive peak near its border to CA1. For illustration, we replotted the frame at 5 ms after stimulation in Figure 8 as a threedimensional profile that shows an increase of the pEPSP along CA3 by a factor of two.

Comparison of distant local recordings. MTA recording allows to correlate local measurements of field potentials at arbitrary positions over large distances. As an example we consider transistor records taken from the representative experiment shown in Figure 5 at the positions marked in Figure 6b. We improved the signal-to-noise ratio by twodimensional spatial Gaussian filtering with $\sigma = \sqrt{2}$ pixel. The transients are plotted in Figure 9. The signal in CA3 (Figure 9a) shows a pEPSP with an amplitude of 4 mV in stratum pyramidale. The pEPSP in CA1 (Figure 9b) is by a factor of two smaller with an amplitude of 2 mV in stratum pyramidale. There is a distinct population spike in CA1 that reflects the firing of pyramidal neurons, but not in CA3 with its higher pEPSP. The experiment reveals a different functionality of pyramidal neurons in two different areas as induced by the same stimulus. The biological implications of the effect have to be studied.

Discussion

Recording of local field potentials. An individual EOMOS transistor records the local electrical field potential in a cultured hippocampus slice at the surface of the substrate, averaged over the area of 16 μm^2 (diameter 4.5µm) of the insulated gate contact. Shape and amplitude of the pEPSP records are similar to signals measured with conventional micropipette electrodes. The fact that EOMOS transistors probe the true field potential is a physical consequence (i) of the direct coupling of the electrical potential from the extracellular space across the insulating electrolyte/chip interface to the transistor gate with an induced change of the source-drain current and (ii) of the proper calibration of the source-drain current by an external modulation of the bath potential (Fromherz 2005). The nature of the measuring process with an EOMOS

transistor is analogous to recording with simple EOS transistors where shape and amplitude of field potentials in cultured hippocampus slices resembled micropipette recordings, too (Besl & Fromherz 2002).

Field potentials in hippocampus slices have been probed by planar metallic multi electrode arrays (MEA) with an electrode diameter of 20-50 µm (area 300-2000 μm^2) and a spacing of 100-200 µm. When we compare the results with MTA recordings, we must consider the same kind of signals. An inspection of reports that refer to pEPSPs in the CA1 or CA3 region of cultured hippocampal slices (Stoppini et al. 1997; Egert et al. 1998; Jahnsen et al. 1999; Duport et al. 1999; Gholmieh et al. 2001; van Bergen et al. 2003) shows that the signal amplitudes were in a range of 400 µV or below. The signal amplitudes in acute slices (Jobling et al. 1981; Novak & Wheeler 1988; Oka et al. 1999; Thiebaud et al. 1999; Heuschkel et al. 2002) were around 200 µV or below. Thus the voltages recorded by planar metal electrodes do not correspond to the field potentials that are measured by micropipette electrodes (Jahnsen et al. 1999). Aspects that may play a role in that discrepancy of MEA recording and that play no role in MTA recording are (i) the chemical inhomogeneity of the substrate (electrodes surrounded by insulator) which may affect the tissue-substrate interaction, (ii) the large size of the metal electrodes that leads to an averaging of the signals and (iii) capacitive shunting of the signals in the extended connection lanes to the amplifier.

Functional imaging in terms of field potentials. MTA recording provides a functional image of slice activity in terms of the field potential on an area of 1 mm^2 at a spatial resolution of 7.8 µm. The high resolution on a large area is important for two kinds of physiological studies.

(i) Field potentials are used to reconstruct the underlying current source density in slices by evaluating the second spatial derivative from discrete sampling (Mitzdorf 1985). However, that procedure is valid only, if the sampling accounts for the highest spatial frequencies in the signal. The linear profile of Figure 7, that is recorded with full spatial resolution, shows that the field potential significantly changes over short distances, within 20 µm by 1 mV or 25% of its amplitude. Thus, the high spatial resolution of MTA recording is crucial if a quantitative current-source density (CSD) analysis is attempted. A CSD analysis on the basis of a sampling of field potentials at intervals of around 100 µm to 200 µm - as provided by common planar multi-electrode arrays - is not adequate.

(ii) Neuronal wiring in a hippocampus slice may give rise to inhomogeneous neuronal activities that change over rather short distances and to correlations of neuronal activity over large distances. Such effects can only be studied, if the activities can be probed at arbitrary positions over a large area. Examples in this report are the modulation of activity along cornu ammonis at the border of CA3 as shown in Figure 8 and the striking difference of postsynaptic signals that are simultaneously recorded at different positions in Figure 9. Such features of spatiotemporal dynamics are difficult to achieve by micropipette electrodes or by coarse sampling with a multi-electrode array.

Compared to planar MEAs, we have to pay for the high spatial resolution on a large area by a lower performance in time resolution of 2 kHz and in noise of 250 µV rms at a full resolution of 7.8 µm and a full recording area of 1000 µm x 1000 µm. Nonetheless, the signal-to-noise ratio is fairly high because the signals are larger by an order of magnitude as compared to MEA recording. However, depending on the problem to be studied, the band width of MTA recording can be enhanced by

lowering the number of pixels that are read out – e.g. with 8 kHz on an area of 500 µm x 500 µm at full spatial resolution –, and subsequent software filtering or/and a spatial averaging over adjacent pixels can be applied, sacrificing spatial resolution. Ongoing improvements of chip design and amplifiers will lead to a significant progress in that respect.

Conclusion

In the present study we implemented a novel neuroelectronic system consisting of a cultured brain slice and a silicon chip with a high-density multi-transistor array (MTA). By direct electrical interfacing of brain slice and chip, we achieved a complete functional image in terms of the field potential on an area of 1 mm^2 at a resolution of 7.8 µm in space and 0.5 ms in time without signal averaging. The test experiments confirm known features of signalling in cultured hippocampal slices. The high density of recording sites and the large area of recording provide time-resolved images of presynaptic and postsynaptic activity that are almost continuous in space. Profiles of field potentials can be evaluated along arbitrary directions. The dynamics of neuronal activity can be correlated over large distances.

Crucial for MTA recording of field potentials is the combination of (i) transistor recording with local probing and calibration of extracellular voltage (Besl & Fromherz 2002), (ii) CMOS technology with a close packing of sensor transistors in two dimensions (Lambacher et al. 2004), and (iii) an inert and homogeneous surface of the silicon chips made of titanium dioxide (Hutzler & Fromherz 2004; Wallrapp & Fromherz 2006). Important for a practical application of MTA recording as a universal electrophysiological tool will be the availability of a chip and a setup that are controlled

by a common PC and also a combination of MTA recording with a multi-capacitor array stimulation. These developments are in progress.

Note. A movie of functional imaging for a cultured hippocampal slice by MTA recording as depicted in Figure 5 is available on the website of the journal. At an enhanced resolution it can be downloaded from the homepage of the Department of Membrane and Neurophysics (www.biochem.mpg.de/mnphys).

Acknowledgments. We thank Michaela Morawetz and Nicole Stöhr for excellent technical assistance, Volker Staiger for advice with electrophysiology, Ralf Zeitler for discussions about the chip measurements, and Erwin Neher for helpful comments on the manuscript.

Grants. The project was supported by the European Union (IST Programme).

References

Amaral DG, Witter MP. The three-dimensional organization of the hippocampal formation: a review of anatomical data. *Neurosci* 31: 571-591, 1989.

Andersen P, Bliss TVP, Skrede KK. Lamellar organization of hippocampal excitatory pathways. *Exp Brain Res* 13: 222-238, 1971.

Besl B, Fromherz P. Transistor array with organotypic brain slice: field potential records and synaptic currents. *Eur J Neurosci* 15: 999-1005, 2002.

Bonhoeffer T, Staiger V, Aertsen A. Synaptic plasticity in rat hippocampal slice cultures: local ”Hebbian“ conjunction of pre- and postsynaptic stimulation leads to distributed synaptic enhancement. *Proc Natl Acad Sci USA* 86: 8113-8117, 1989.

Caesar M, Aertsen A. Morphological organization of rat hippocampal slice cultures. *J Comp Neurol* 307: 87-106, 1991.

Davies J, Watkins JC. Actions of D and L forms of 2-amino-5-phosphonovalerate and 2-amino-4-phosphonobutyrate in the cat spinal cord. *Brain Res* 235: 378-386, 1982.

Debanne D, Gähwiler BH, Thompson SM. Heterogeneity of synaptic plasticity at unitary CA3-CA1 and CA3-CA3 connections in rat hippocampal slice cultures. *J Neurosci* 19: 10664-10671, 1999.

Duport S, Millerin C, Muller D, Correges P. A metallic multisite recording system designed for continuous long-term monitoring of electrophysiological activity in slice cultures. *Biosens Bioel* 14: 369-376, 1999.

Egert U, Schlosshauer B, Fennrich S, Nisch W, Fejtl M, Knott T, Müller T, Hämmerle H. A novel organotypic long-term culture of the rat hippocampus on substrate-integrated multielectrode arrays. *Brain Res Prot* 2: 229-242, 1998.

Eversmann B, Jenkner M, Paulus C, Hofmann F, Brederlow R, Holzapfl B Fromherz P, Brenner M, Schreiter M. Gabl R, Plehnert K, Steinhauser M, Eckstein G, Schmitt-Landsiedel D. Thewes R. A 128 x 128 CMOS biosensor array for extracellular recording of neural activity, *IEEE J Solid State Circuits* 38: 2306-2317, 2003.

Fromherz P. Sheet conductor model of brain slices for stimulation and recording with planar electronic contacts. *Eur Biophys J* 31: 228-231, 2002.

Fromherz P. The Neuron-Semiconductor Interface. In: *Bioelectronics- from theory to applications*, edited by Willner I, Katz E: Weinheim:Wiley-VCH, 2005.

Gähwiler BH. Organotypic monolayer cultures of nervous tissue. *J Neurosci Meth* 4: 329-342, 1981.

Gholmieh G, Soussou W, Courellis S, Marmarelis V, Berger T, Baudry M. A biosensor for detecting changes in cognitive processing based on nonlinear systems analysis. *Biosens Bioel* 16:491-501, 2001.

Grinvald A, Hildesheim R. VSDI: A new era in functional imaging of cortical dynamics. *Nature Rev Neurosci* 5: 874-885, 2004.

Grinvald A, Manker A, Segal M. Visualization of the spread of electrical activity in rat hippocampal slices by voltage-sensitive optical probes. *J Physiol* (London) 333:

269-291, 1982.

Heuschkel MO, Fejtl M, Raggenbass M, Bertrand D, Renaud P. A three-dimensional multi-electrode array for multi-site stimulation and recording in acute brain slices. *J Neurosci Meth* 114: 135-148, 2002.

Honore T, Davies SN, Dreyer J, Fletcher EJ, Jacobsen P, Lodge D, Nielsen FE. Quinoxalin-diones: potent competitive non-NMDA glutamate receptor antagonists. *Science* 241: 701-703, 1988.

Hutzler M, Fromherz P. Silicon chip with capacitors and transistors for interfacing organotypic brain slice of rat hippocampus. *Eur J Neurosci 19*: 2231-2238, 2004.

Ishizuka N, Weber J, Amaral DG. Organization of intrahippocampal projections originating from CA3 pyramidal cells in the rat. *J Comp Neurol* 295: 580-623, 1990.

Jahnsen H, Kristensen BW, Thiebaud P, Noraberg J, Jacobsen B, Bove M, Martinoia S, Koudelka-Hep M, Grattarola M, Zimmer J. Coupling of organotypic brain slice cultures to silicon-based arrays of electrodes. *Methods* 18: 160-172, 1999.

Jobling DT, Smith JG, Wheal HV. Active microelectrode array to record from the mammalian central nervous-system invitro. *Med Biol Eng & Comput* 19: 553-560, 1981.

Johnston D, Amaral DG. Hippocampus. In: *The synaptic organization of the brain*, edited by Shepherd G M: Oxford, Oxford UP, 1998

Lambacher A, Jenkner M, Merz M, Eversmann B, Kaul RA, Hofmann F, Thewes R, Fromherz P. Electrical imaging of neuronal activity by multi-transistor-array

(MTA) recording at 7.8 μm resolution. *Appl Phys A* 79: 1607-1611, 2004.

Mann EO, Suckling JM, Hajoos N, Greenfield SA, Paulsen O. Perisomatic feedback inhibition underlies cholinergically induced fast network oscillations in the rat hippocampus in vitro. *Neuron* 45: 105-117, 2005.

Matsukawa H, Wolf AM, Matsushita S, Joho RH, Knöpfel T. Motor dysfunction and altered synaptic transmission at the parallel fiber – Purkinje cell synapse in mice lacking potassium channels Kv3.1 and Kb3.3. *J Neurosci* 23: 7677-7684, 2003.

Meister M, Wong ROL, Baylor DA, Shatz CJ. Synchronous bursts of action potentials in ganglion cells of the developing mammalian retina. *Science* 252: 939-943, 1991.

Mitzdorf U. Current-source density method and application in cat cerebral cortex: investigation of evoked field potentials and EEG phenomena. *Physiol Rev* 65: 37-100, 1985.

Nakagami Y, Saito H, Matsuki N. Optical recording of trisynaptic pathway in rat hippocampals slices with a voltage-sensitive dye. *Neurosci* 81: 1-8, 1997.

Novak J, Wheeler B. Multisite hippocampal slice recording and stimulation using a 32 element microelectrode array. *J Neurosci Meth* 23: 149-159, 1988.

Oka H, Shimono K, Ogawa R, Sugihara H, Taketani M. A new planar multielectrode array for extracellular recording: application to hippocampal acute slice. *J Neurosci Meth* 93 : 61-67, 1999.

Ramón y Cajal S *Histologie du Système Nerveux de l´Homme et des Vertèbres*. Paris:

Maloine, 1911.

Richardson T, Turner R, Miller J. Action potential discharge in hippocampal CA1 pyramidal neurons: current source-density analysis. *J. Neurophysiol.* 58: 981-995, 1987.

Segev R, Goodhouse J, Puchalla J, Berry MJ. Recording spikes from a large fraction of the ganglion cells in a retinal patch. *Nature Neurosci* 7: 1155-1162, 2004.

Stoppini L, Duport S, Correges P. A new extracellular multirecording system for electrophysiological studies: application to hippocampal organotypic cultures. *J Neurosci Meth* 72: 23-33, 1997.

Thiebaud P, Beuret C, Koudelka-Hep M, Bove M, Martinoia S, Grattarola M, Jahnsen H, Rebaudo R, Balestrino M, Zimmer J, Dupont Y. An array of Pt-tip microelectrodes for extracellular monitoring of activity of brain slices. *Biosens Bioel* 14: 61-65, 1999.

Van Bergen A, Papanikolaou T, Schuker A, Moller A, Schlosshauer B. Long-term stimulation of mouse hippocampal slice culture on microelectrode array. *Brain Res Prot* 11: 123-133, 2003.

Wallrapp F, Fromherz P. TiO_2 and HfO_2 in electrolyte-oxide-silicon configuration for applications in bioelectronics. *J Appl Phys* in press, 2006

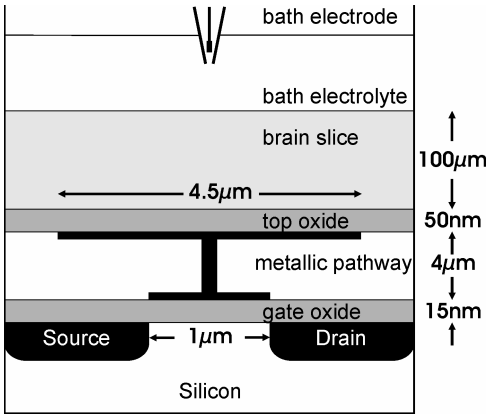

Figure 1. Schematic cross section of a sensor transistor with electrolyte-oxide-metal-oxide-silicon (EOMOS) configuration (not to scale). The brain slice is in contact to a top layer of titanium dioxide that is connected by a metallic pathway to the gate oxide of a field-effect transistor with source and drain.

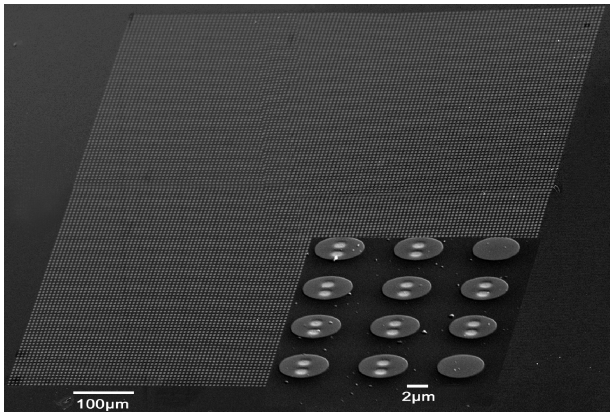

Figure 2. Surface of multi-transistor array (MTA). Scanning electronmicrograph. The array consists of 128x128 sensor transistors on 1 mm^2 with a pitch of 7.8 µm. The surface is made of a chemically homogeneous and electrically insulating layer of titanium dioxide. The insert shows a blow up. The upper gate contacts of the sensor transistors (diameter of 4.5 µm, platinum on two tungsten pins) shine through the oxide layer.

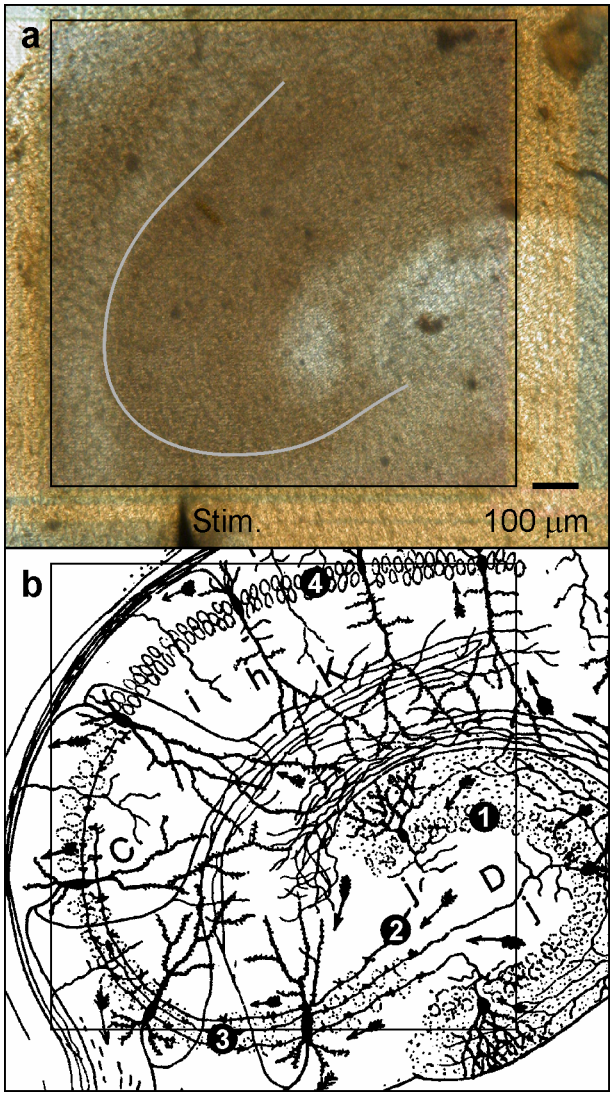

Figure 3. Multi-transistor array (MTA) and rat hippocampus. (a) Micrograph of cultured slice on silicon chip. The area of the MTA (1 mm x 1 mm) is marked by a black frame. The grey line marks the border between positive and negative amplitude of postsynaptic field potentials as measured with the MTA (see Figure 6). The brighter field to the left is stratum pyramidale. The black triangle at the bottom is the stimulation electrode. (b) For comparison, the classical drawing of a Golgi stained section of rat hippocampus (Ramón y Cajal 1911) is matched in orientation and size. The frame marks the approximate area observed by the MTA. Gyrus dentatus (1), mossy fibers (2), stratum pyramidale of CA3 (3) and of CA1 (4) are labelled.

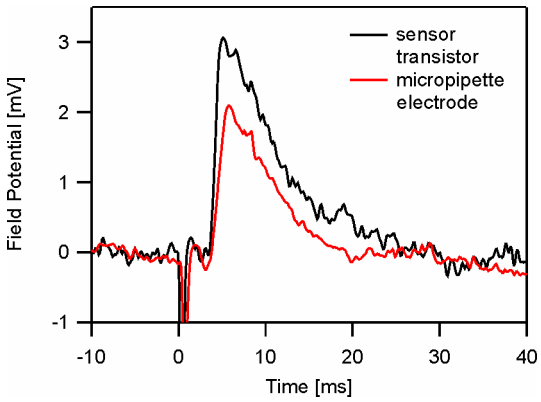

Figure 4. Comparison of transistor record and micropipette record. Transistor signal (black) and micropipette signal (red) versus time in stratum pyramidale of a cultured brain slice after stimulation with a tungsten microelectrode at time t=0. Spatial Gaussian filtering of the transistor signal with $\sigma = \sqrt{2}$ pixel. The tip of the pipette is close to the position of the transistor, slighly above the surface of the chip.

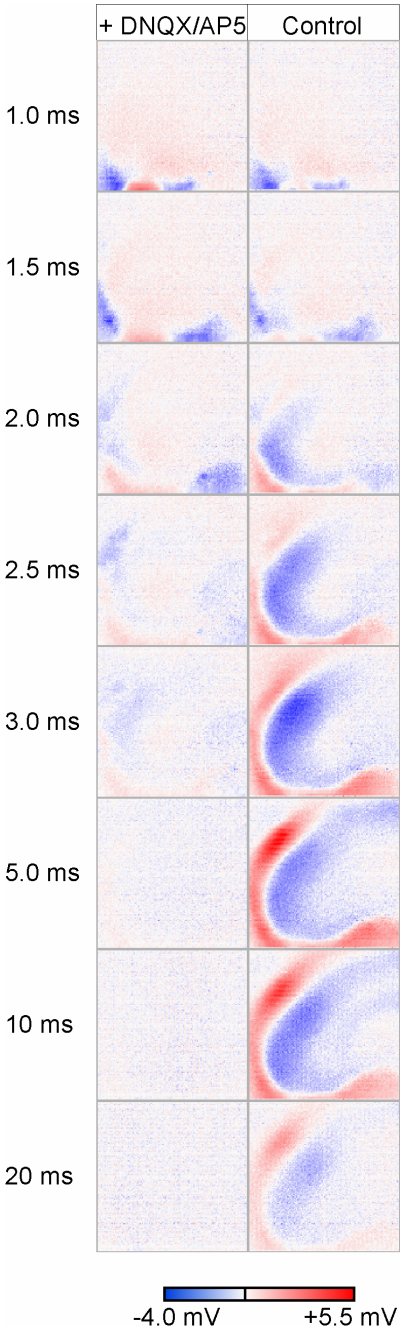

Figure 5. Time resolved images of field potential in cultured hippocampal slice measured by a MTA. Recording area 1 mm x 1 mm. Eight frames are selected at different times after stimulation in stratum pyramidale of CA3 region with a tungsten microelectrode (see Figure 3a). Left column: slice perfused with recording medium containing DNQX and AP5. Right column: slice perfused with normal recording medium. Color code at the bottom. A movie of the complete dynamics can be downloaded from the homepage of the journal.

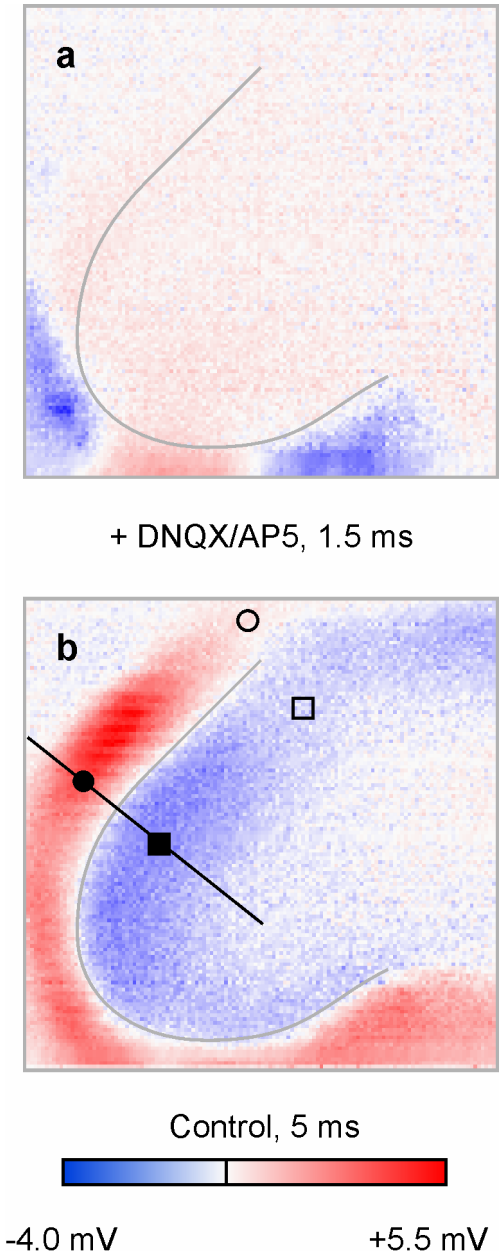

Figure 6. Comparison of early and late field potentials. (a) Field potential with toxins DNQX and AP5 1.5 ms after stimulation. (b) Field potential without toxins 5 ms after stimulation. Color code at the bottom. The grey line marks the border between positive and negative signals in b. A linear section is marked where profiles of field potential are plotted in Figure 7. Four positions are marked where complete time dependent records are shown in Figure 9.

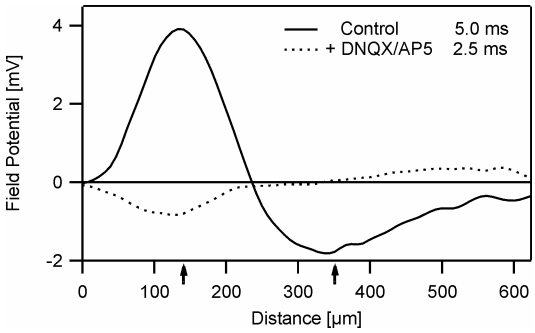

Figure 7. One-dimensional profiles of field potential evaluated at full spatial resolution from the data set of Figure 5. The position of the profiles is marked in Figure 6b. Solid line: without toxins 5 ms after stimulation. Dotted line: with toxins 2.5 ms after stimulation. Spatial Gaussian filtering with $\sigma = \sqrt{2}$ pixel. The arrows mark the position of the local records in Figure 9a.

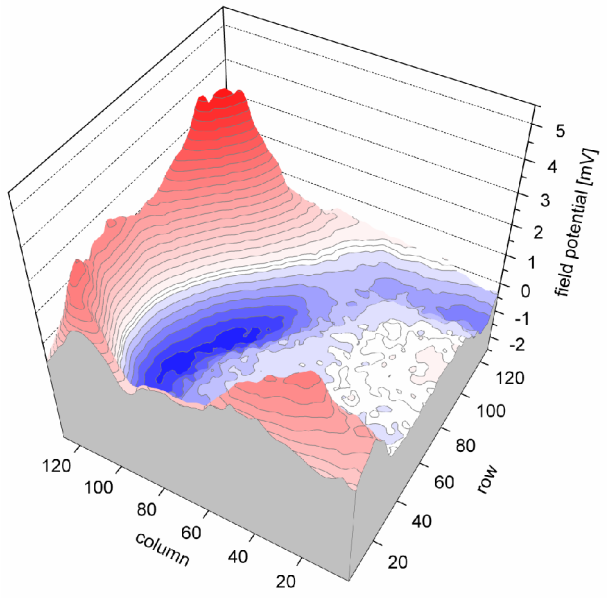

Figure 8. Isochronic threedimensional profile of field potential without toxins 5 ms after stimulation. The 128x128 sensor transistors cover 1 mm^2 of a cultured slice. The profile corresponds to the 5 ms picture in Figure 5 (right column).

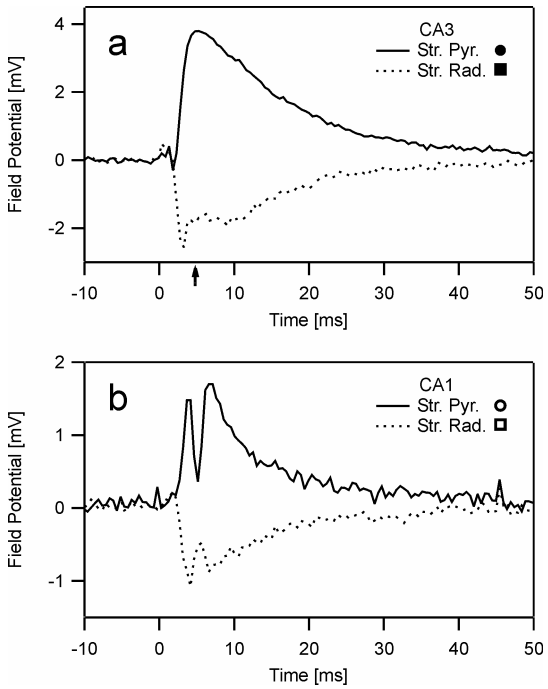

Figure 9. Local dynamics of field potentials without toxins in CA3 and CA1. (a) Transistor records in CA3 for stratum pyramidale (full line) and stratum radiatum (dashed line) at locations marked in Figure 6b with black symbols. The arrow marks the time of the profile in Figure 7. (b) Transistor records in CA1 at locations marked in Figure 6b with bright symbols. The data are filtered by a twodimensional Gaussian with $\sigma = \sqrt{2}$ pixel, after removal of stimulus artifacts.